

Optical Constants of Rubidium and Cesium from 0.5 to 4.0 eV[†]

Neville V. Smith

Bell Telephone Laboratories, Murray Hill, New Jersey 07974 and Stanford, University, Stanford, California 94305*

(Received 7 May 1970)

Measurements are reported for ϵ_1 and ϵ_2 , the real and imaginary parts of the dielectric constant, of Rb and Cs at room temperature in the frequency range 0.5–4.0 eV. The experiments were performed by multiple reflection at metal-silica interfaces employing the technique used earlier on Na and K. The optical absorption of Rb shows structure which can be attributed to conventional interband transitions within the nearly free-electron model. The optical absorption of Cs also shows structure, but the threshold occurs at a lower frequency than that predicted by the nearly free-electron model. Both metals show a leveling off and a perceptible rise in the absorption at the high-frequency end of the range. The possibility of absorption due to many-body effects or transitions to d bands above the Fermi level is discussed. The results for ϵ_1 are used to deduce values for the infrared optical masses which are found to be 1.16 m for Rb and 1.19 m for Cs.

I. INTRODUCTION

The experimental techniques used by the author in recent measurements of the optical constants¹ of Na and K have been extended to Rb and Cs. Results are presented here for ϵ_1 and ϵ_2 , the real and imaginary parts of the dielectric constant, obtained on thick films of Rb and Cs at room temperature in the frequency range 0.5–4.0 eV. The measurements were performed by multiple reflection at interfaces between the alkali metal and fused silica. The results will be compared with the predictions of the nearly free-electron model, with the data of previous workers, and with the results obtained on the other alkali metals.

A main feature of the results¹ for the optical conductivity $\sigma(\omega)$ on Na and K was the general agreement with the predictions of the nearly free-electron model. This was in contrast with the previous results of Mayer and collaborators^{2,3} who had found anomalous peaks at frequencies below the interband threshold. It will be seen that the optical conductivity of Rb is similar to that of Na and K. Structure is found in the frequency dependence of $\sigma(\omega)$ which can be attributed to conventional interband transitions associated with the $\langle 110 \rangle$ reciprocal-lattice vectors. The threshold occurs near the free-electron value of $0.64E_F$, where E_F is the free-electron Fermi energy.

The values of $\sigma(\omega)$ for Cs also show structure but the threshold is significantly lower than $0.64E_F$. This suggests that a nearly free-electron approach is inappropriate for Cs since the introduction of gaps at the zone boundaries should, if anything, increase the threshold frequency above the free-electron value. It is conjectured that the behavior in Cs is associated with the existence of flat d -like bands just above the Fermi level.

At higher frequencies, it will be seen that the values for $\sigma(\omega)$ in K, Rb, and Cs are found to level off and then start to rise again, indicating the onset of some new absorption. The beginning of the rise occurs in the vicinity of the plasma frequency. The extra absorption may therefore be due to one of the plasmon-induced processes which have been proposed recently. Alternatively, the extra absorption may be due to transitions to unoccupied d bands which are believed to exist not too far above the Fermi level in the heavier alkali metals.

The results for ϵ_1 have been used to deduce values for the optical masses in Rb and Cs. First of all, a correction was made for ϵ_{1i} , the interband contribution to ϵ_1 , by a Kramers-Krönig inversion of the interband absorption found in $\sigma(\omega)$. This proved to be particularly necessary in Cs where the absorption is much larger than in the other alkali metals and occurs at lower frequencies. In Sec. V, the infrared optical masses of Li, Na, K, Rb, and Cs will be compared with Ham's theoretical band masses and with the masses obtained in electronic specific-heat and cyclotron-resonance experiments.

II. EXPERIMENTAL TECHNIQUE

The measurements were made by multiple reflection at metal-silica interfaces using a split-beam ellipsometer and a null procedure whose details have been described earlier.¹ Monochromatic light was passed down a long narrow plate of fused silica and reflected internally seven times. The geometry of the arrangement is illustrated schematically in Fig. 1. The alkali-metal sample was deposited on both sides of the plate by evaporation from the ampoules also shown in Fig. 1. The plates were made of $\frac{1}{8}$ -in.-thick stock-polished Suprasil. The

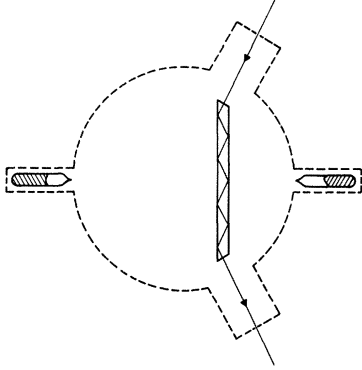


FIG. 1. Schematic diagram of the optical system and vacuum chamber, showing position of fused-silica plate and the ampoules containing the alkali-metal sample.

angle of incidence at each reflection was 75° , and the entrance and exit faces were cut so as to be normal to the beam.

It was shown in the earlier work that the multiple-reflection technique has special advantages in cases such as the alkali metals where the optical absorption is small. The cumulative effect of several reflections is to boost the total absorption and make it more measurable. Any structure in the frequency dependence of the absorption becomes particularly more pronounced. During the course of the work, it came to the author's attention that multiple-internal-reflection spectroscopy has enjoyed considerable use by physical chemists and has recently been the subject of an interesting book by Harrick.⁴ The combination of ellipsometry and multiple-internal-reflection spectroscopy, however, does not seem to have been widely used.

The samples were thick films prepared by evaporation in an ultrahigh vacuum system described elsewhere by Smith and Spicer.⁵ The alkali-metal samples were obtained already sealed under vacuum in glass ampoules.⁶ The quoted purities were 99.95% for Rb and 99.97% for Cs. The ampoules were kept intact during the pumpdown and bakeout of the vacuum system. They were then broken open and the subsequent burst of gas pumped away. Pressures lower than 5×10^{-11} Torr were reached by the following day. The evaporations were performed by gently heating the ampoules from outside the chamber and took from $\frac{1}{2}$ to 1 h. As in the work on Na and K, the ellipsometric parameters were monitored, and the evaporations were continued until well after the interference oscillations due to multiple reflections within the films had died away and until no further changes occurred on adding more material. Rb and Cs are both fairly volatile metals, and it was found that after a con-

siderable amount of metal had been released into the chamber, the pressure gradually rose and leveled off at the room-temperature vapor pressure.

The values obtained for ϵ_1 and ϵ_2 on Rb and Cs are listed for a range of photon energies between 0.5 and 4.0 eV in Tables I and II. Also listed are the values for the optical conductivity σ and the normal reflectivity R . These quantities were calculated from the measured ϵ_1 and ϵ_2 using the following standard formulas:

$$\sigma = \omega \epsilon_2 / 4\pi, \quad (1)$$

$$R = [(n-1)^2 + k^2] / [(n+1)^2 + k^2], \quad (2)$$

where

$$n - ik = (\epsilon_1 - i\epsilon_2)^{1/2}. \quad (3)$$

These results are discussed and interpreted in Secs. III and IV. The experimental accuracy is much the same as that in the previous work on Na and K. For example, the estimated limits of error in the values of $\sigma(\omega)$ listed in Tables I and II are typically $\pm 0.04 \times 10^{14} \text{ sec}^{-1}$.

III. OPTICAL CONDUCTIVITY

According to elementary theory, the optical conductivity can be expressed as the sum of a Drude free-carrier term $\sigma_D(\omega)$ and an interband term $\sigma_i(\omega)$,

$$\sigma(\omega) = \sigma_D(\omega) + \sigma_i(\omega). \quad (4)$$

The Drude contribution is given by

$$\sigma_D(\omega) = Ne^2 / m^* \omega^2 \tau, \quad (5)$$

where N is the density of conduction electrons, τ is a relaxation time,⁷ and m^* is an effective mass. For nearly free-electron monovalent metals, the interband contribution may be expressed in the following form derived by Wilson⁸ and by Butcher⁹:

$$\sigma_i(\omega) = \frac{me^2}{\pi \hbar^4} \frac{|V_G|^2}{G} \frac{(\omega_{hi} - \omega)(\omega - \omega_{lo})}{\omega^3}, \quad \omega_{lo} < \omega < \omega_{hi} \\ = 0, \text{ elsewhere.} \quad (6)$$

The low- and high-frequency thresholds are given by

$$\hbar \omega_{lo} = (\hbar^2 / 2m) (G - 2k_F)G, \quad (7)$$

$$\hbar \omega_{hi} = (\hbar^2 / 2m) (G + 2k_F)G. \quad (8)$$

\vec{G} is a reciprocal-lattice vector, and is taken to be the $[110]$ vector \vec{G}_{110} in the alkali metals which have the bcc structure. Since $G_{110}/2k_F = 1.14$, we are led to the following useful relation between $\hbar \omega_{lo}$ and E_F , the free-electron Fermi energy:

$$\hbar \omega_{lo} = 0.64 E_F. \quad (9)$$

For Rb, $\hbar \omega_{lo}$ has the value 1.14 eV, and for Cs it

TABLE I. Optical constants of rubidium.

$\hbar\omega$ (eV)	ϵ_1	ϵ_2	$\sigma(\omega)$ (10^{14} (sec $^{-1}$))	R
0.554	-39.74	2.174	1.457	0.9832
0.570	-38.10	1.994	1.375	0.9836
0.585	-36.21	1.865	1.319	0.9835
0.626	-31.13	1.487	1.126	0.9835
0.674	-26.84	1.266	1.032	0.9826
0.734	-22.13	1.026	0.911	0.9813
0.810	-17.88	0.818	0.801	0.9797
0.922	-13.44	0.669	0.746	0.9750
1.055	-9.87	0.564	0.720	0.9675
1.228	-7.05	0.478	0.711	0.9563
1.442	-5.09	0.457	0.798	0.9357
1.653	-3.50	0.408	0.816	0.9080
1.873	-2.51	0.346	0.784	0.8834
2.067	-1.893	0.280	0.701	0.8696
2.271	-1.444	0.241	0.666	0.8490
2.455	-1.101	0.204	0.606	0.8324
2.638	-0.810	0.177	0.567	0.8063
2.818	-0.616	0.160	0.546	0.7799
2.952	-0.416	0.148	0.531	0.7279
3.064	-0.267	0.139	0.516	0.6658
3.204	-0.160	0.135	0.523	0.5872
3.397	0.005	0.127	0.523	0.3728
3.711	0.192	0.127	0.570	0.1442
3.967	0.285	0.124	0.595	0.0909

is 0.97 eV. Let us compare these simple theoretical predictions with the experimental results.

The experimental values for $\sigma(\omega)$ in Rb are shown in Fig. 2 as full circles. The full curve represents the total absorption predicted theoretically in Eqs. (4)–(6). The individual contributions are indicated by the dashed curves. The relaxation time used in the Drude contribution was calculated from the

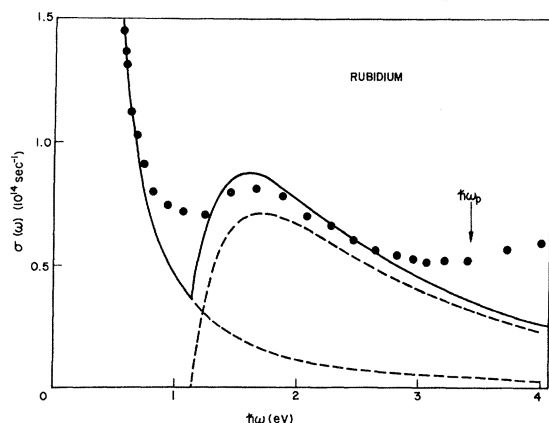


FIG. 2. Optical conductivity of rubidium. The full circles represent the experimental values. The full curve is the theoretical prediction of the nearly free-electron model with $|V_{110}| = 0.26$ eV, and the dashed curves represent the individual Drude and interband contributions.

known dc conductivity σ_0 by means of the relation $\tau = \sigma_0 m^* / Ne^2$. m^* was taken to be equal to the bare mass m in this calculation. In the interband contribution, $|V_{110}|$ was taken to be 0.26 eV. This value was chosen to give a total $\sigma(\omega)$ whose magnitude was tolerably close to the experimentally measured magnitude in the vicinity of the peak at around $\hbar\omega = 1.6$ eV in Fig. 2. The experimental $\sigma(\omega)$ is in at least qualitative agreement with the theoretical prediction in that it does show structure at the expected frequency. The threshold in the experimental $\sigma(\omega)$, however, is nowhere near as sharp as that predicted at 1.14 eV. The observed values for $\sigma(\omega)$ below this frequency are larger than the calculated Drude values. In these respects, the behavior of Rb is much the same as that observed earlier in Na and K.¹

The corresponding results for Cs are shown in Fig. 3. As in Rb, the experimental values for $\sigma(\omega)$ show a threshold and a peak, but these occur at much lower frequencies than those predicted theoretically. The theoretical threshold occurs at 0.97 eV and the peak at about 1.4 eV. In experiment, the threshold occurs between 0.6 and

TABLE II. Optical constants of cesium.

$\hbar\omega$ (eV)	ϵ_1	ϵ_2	$\sigma(\omega)$ (10^{14} (sec $^{-1}$))	R
0.512	-34.70	3.097	1.918	0.9711
0.572	-26.50	2.506	1.734	0.9654
0.587	-25.36	2.431	1.726	0.9642
0.608	-23.58	2.397	1.763	0.9609
0.626	-21.99	2.242	1.698	0.9595
0.651	-20.58	2.278	1.794	0.9548
0.675	-18.75	2.232	1.820	0.9496
0.702	-17.47	2.217	1.883	0.9447
0.734	-16.06	2.190	1.944	0.9386
0.777	-14.14	2.109	1.982	0.9294
0.818	-12.62	2.054	2.032	0.9197
0.864	-11.53	2.034	2.126	0.9103
0.923	-9.76	1.922	2.146	0.8941
1.046	-7.47	1.742	2.204	0.8639
1.219	-5.45	1.502	2.215	0.8250
1.400	-3.84	1.200	2.032	0.7851
1.625	-2.65	0.924	1.847	0.7435
1.842	-1.786	0.725	1.609	0.6924
2.033	-1.265	0.602	1.481	0.6430
2.226	-0.900	0.517	1.393	0.5898
2.417	-0.653	0.465	1.360	0.5353
2.638	-0.375	0.414	1.322	0.4399
2.818	-0.209	0.387	1.319	0.3588
2.952	-0.050	0.367	1.311	0.2625
3.100	0.035	0.353	1.325	0.2110
3.204	0.148	0.339	1.314	0.1475
3.351	0.226	0.337	1.367	0.1114
3.397	0.282	0.321	1.320	0.0902
3.711	0.427	0.310	1.392	0.0501
3.967	0.656	0.288	1.381	0.0177

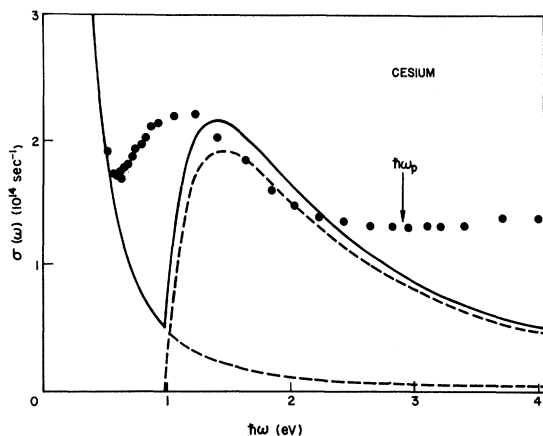


FIG. 3. Optical conductivity of cesium. The full circles represent the experimental values. The full curve is the theoretical prediction of the nearly free-electron model with $|V_{110}| = 0.38$ eV, and the dashed curves represent the individual Drude and interband contributions.

0.7 eV and the peak at about 1.1 eV. These discrepancies represent a serious failure of the nearly free-electron approach. The discrepancy cannot be explained by taking fuller account of the gaps at the zone boundaries. Opening up a gap will tend to widen the separation between the bands and therefore increase the threshold frequency. For example, Ham¹⁰ estimates the threshold to be at 1.3 eV, and Ashcroft¹¹ places it at 1.36 eV.

One possibility for the behavior in Cs is that the upper band in the optical transitions is flat, possibly a *d* band. The existence of flat *d*-like bands in the heavier alkali metals not far above the Fermi level is readily apparent in Ham's band calculations.¹² These *d* bands become closer to the Fermi level as one proceeds across the series from K to Rb to Cs. In fact, Ham's calculations on Cs indicate that if the lattice parameter is slightly reduced, the *d*-like state at N_2 can actually interpose itself into the band gap between the *s*- and *p*-like states at N_1 , and N_1 . We suggest, therefore, that the low value of the threshold in Cs is due to optical transitions from the Fermi level to a flat low-lying excited band, possibly the *d*-like Σ_2 band which has somehow been depressed so that it lies between the *s*- and *p*-like Σ_1 bands. (The reader is referred to Figs. 5–7 of Ham's paper¹² for further illustration of this hypothesis.) It is worth noting that the proximity of the upper *d* bands in Cs has been invoked before to explain the maximum in the pressure dependence of the electrical resistivity.¹³

In both Rb and Cs, there is a notable discrepancy between theory and experiment at the high-energy end of the frequency range. The theoretical values for $\sigma(\omega)$ in Figs. 2 and 3 show a steady decrease

with increasing frequency. The experimental points, however, show a definite leveling off and a perceptible rise at the very highest frequencies, indicating some extra absorption. The locations of the respective plasma frequencies taken from Kunz¹⁴ have been indicated in Figs. 2 and 3. It can be seen that the onset of the additional absorption starts in the vicinity of the plasma frequency. It is possible that we are observing one or more of the plasmon-induced absorption mechanisms proposed by Hopfield,¹⁵ by Esposito, Muldower and Bloomfield,¹⁶ and by Hedin, Lundqvist, and Lundqvist.¹⁷ An alternative explanation is that the extra absorption is due to higher interband transitions. It has already been mentioned that the heavier alkali metals are believed to have flat *d*-like bands lying not too far above the Fermi level. If this explanation is correct, the occurrence of the extra absorption near the plasma frequency would then be coincidental.

The new results for $\sigma(\omega)$ in Rb and Cs are compared with the results of previous workers in Figs. 4 and 5. The results of von Aufschnaiter¹⁸ on Rb agree reasonably well with the author's as far as over-all magnitude of the absorption is concerned, but do not show the structure which we have attributed to interband transitions. The absorption measured by Ives and Briggs¹⁹ on Rb is significantly higher than the more recent results.

In Cs, there is qualitative agreement at low frequencies between the present work and the results of Mayer and Hietel.³ Both sets of data indicate that the threshold in $\sigma(\omega)$ occurs between 0.6 and 0.7 eV and that the peak occurs at about 1.1 eV. The quantitative agreement at low frequencies is not good. At the higher frequencies, on the other hand, there is excellent agreement between the author's data, Mayer and Hietel's data,³ and the

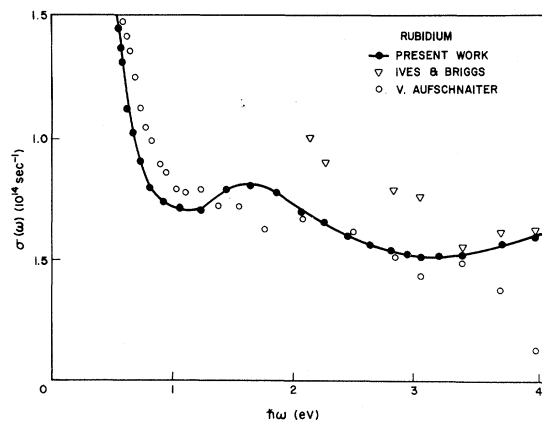


FIG. 4. Optical conductivity of rubidium: Comparison with results of previous workers.

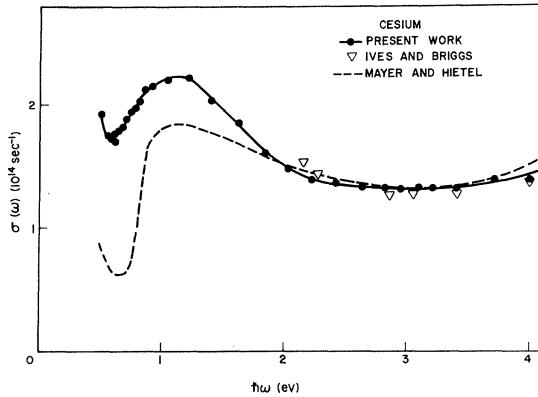


FIG. 5. Optical conductivity of cesium: Comparison with results of previous workers.

data of Ives and Briggs.¹⁹ There are, therefore, three independent sets of measurements of $\sigma(\omega)$ on Cs in the visible and ultraviolet which are in close agreement. In particular, each set of measurements shows the leveling off and gradual rise at the end of the range mentioned earlier. We may regard this feature of the absorption in Cs as well established.

IV. REAL PART OF DIELECTRIC CONSTANT

The real part of the dielectric constant may be expressed as follows²⁰:

$$\epsilon_1 = 1 + 4\pi N\alpha_0 - Ne^2\lambda^2/m^*\pi c^2 + \epsilon_{1i}. \quad (10)$$

The term $4\pi N\alpha_0$ represents the core polarizability and may be regarded as a constant whose magnitude is of order 0.1. The third term involving λ , the free-space wavelength of the light, is the dominant term and is due to the response of the conduction electrons. A plot of the experimental ϵ_1 against λ^2 should give a straight line whose slope will yield a value for the quantity m^* usually known as the optical mass. The fourth term, ϵ_{1i} is the contribution to ϵ_1 due to interband transitions. Although this term is small, it varies appreciably in Rb and Cs over the experimental frequency range and can lead to errors in the values obtained for m^* if no correction is made for it. This turns out to be particularly true in the case of Cs. The correction is very straightforward to make, using the Kramers-Krönig relations which we write as follows:

$$\epsilon_{1i}(\omega) = 8 \int_0^{\omega_0} \frac{\sigma_i(x) dx}{x^2 - \omega^2} + 8 \int_{\omega_0}^{\infty} \frac{\sigma_i(x) dx}{x^2 - \omega^2}. \quad (11)$$

The integral over frequency has been separated into two parts at the frequency ω_0 . Provided we confine our attention to frequencies for which $\omega \ll \omega_0$, the second integral may be treated as a

constant whose value cannot affect the slope of a plot of ϵ_1 versus λ^2 . The first integral was calculated numerically for both Rb and Cs. The values used for $\sigma_i(\omega)$ were obtained by subtracting the Drude curves shown in Figs. 2 and 3 from the experimental values of $\sigma(\omega)$. The truncation frequency, ω_0 was taken at 4 eV, the upper limit of the experimental measurements. The value of the second integral was neglected.

The experimental values of $-\epsilon_1$ for Rb are shown as full circles plotted against λ^2 in Fig. 6. The open circles represent the values of $-(\epsilon_1 - \epsilon_{1i})$ where ϵ_{1i} , the correction factor for interband transitions, was calculated according to the prescription outlined above. A straight line was fitted to the open circles, and its slope gave a value for the optical mass equal to 1.16 m. In Rb, the correction ϵ_{1i} turns out to be small and does not significantly affect the value obtained for the optical mass. The correction is found to be even smaller in Na and K, and this justifies its neglect in the previous

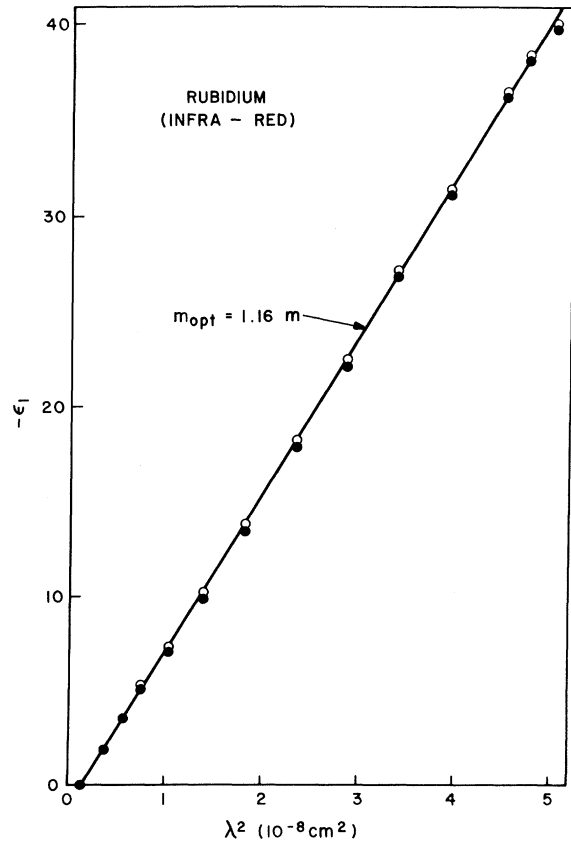


FIG. 6. Real part of the dielectric constant of rubidium in the infrared. The full circles represent the measured values. The open circles contain a Kramers-Krönig correction for the interband contribution.

paper.¹

The experimental values for $-\epsilon_1$ in Cs are shown in Fig. 7. Once again, the open circles represent the corrected quantity $-(\epsilon_1 - \epsilon_{1i})$. It is seen that the correction in Cs is quite significant. The value of the optical mass obtained from the corrected points is 1.19 m. If no correction had been made, the value would have been 1.30 m. This is consistent with an argument presented in the previous paper where it was shown that the uncorrected optical mass is expected to be greater than m^* within an interband frequency region. We will refer to m^* as the infrared optical mass, i.e., the optical mass which would be obtained at frequencies well below the interband threshold where ϵ_{1i} becomes constant. The limits of error in the quoted values for m^* are estimated to be 2-3%.

It was also shown in the previous paper that at sufficiently high frequencies, the behavior of ϵ_{1i} causes the graph of $-\epsilon_1$ versus λ^2 to return to a steeper slope, giving an uncorrected optical mass which is less than m^* . The short-wavelength results for $-\epsilon_1$ in Rb and Cs are plotted in Figs. 8 and 9. The dashed lines are continuations of the lines shown in Figs. 6 and 7. The experimental

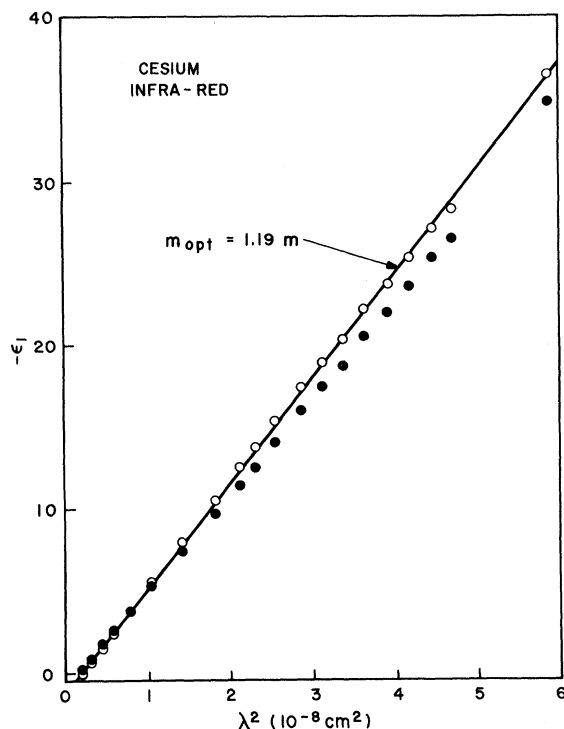


FIG. 7. Real part of the dielectric constant of cesium in the infrared. The full circles represent the measured values. The open circles contain a Kramers-Krönig correction for the interband contribution.

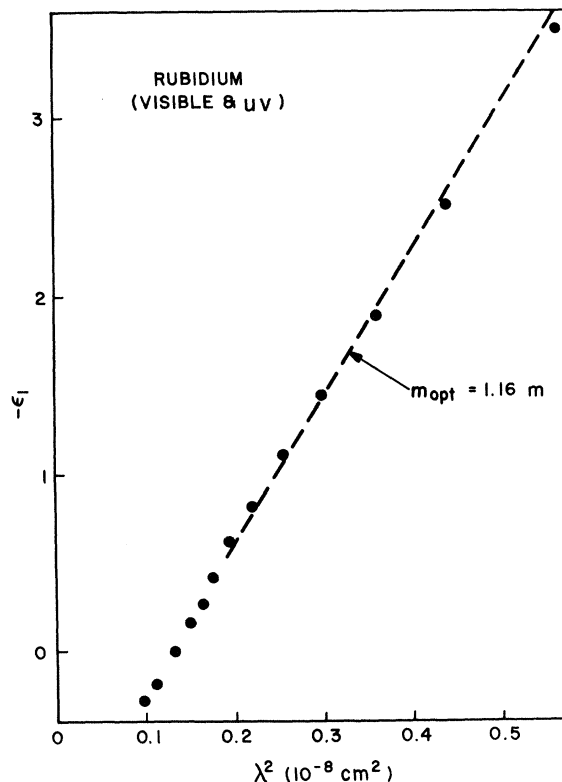


FIG. 8. Real part of the dielectric constant of rubidium in the visible and near ultraviolet. The dashed line is a continuation of the line in Fig. 6.

points do indeed return to a steeper slope at the shortest wavelengths. Part of this steepening may be due to structure in $\sigma(\omega)$ at even shorter wavelengths. It was noted in Figs. 2 and 3 that there is evidence for such structure.

The wavelength at which the experimental points cross the $\epsilon_1 = 0$ axis gives values for the plasma frequency. These were found to be 3.4 eV for Rb and 3.0 eV for Cs. These agree reasonably well with the values of 3.41 and 2.9 eV, respectively, determined by Kunz¹⁴ from characteristic energy-loss experiments.

V. COMPARISON WITH OTHER ALKALI METALS

A. Optical Conductivity

The optical conductivity measurements made by the author on four alkali metals Na, K, Rb, and Cs are compared in Fig. 10. They have been plotted against the normalized frequency $\hbar\omega/E_F$ where E_F is the free-electron Fermi energy. According to Eq. (9), the free-electron value of the low-frequency threshold occurs at 0.64 on this scale and is indicated by the broken vertical line in Fig.

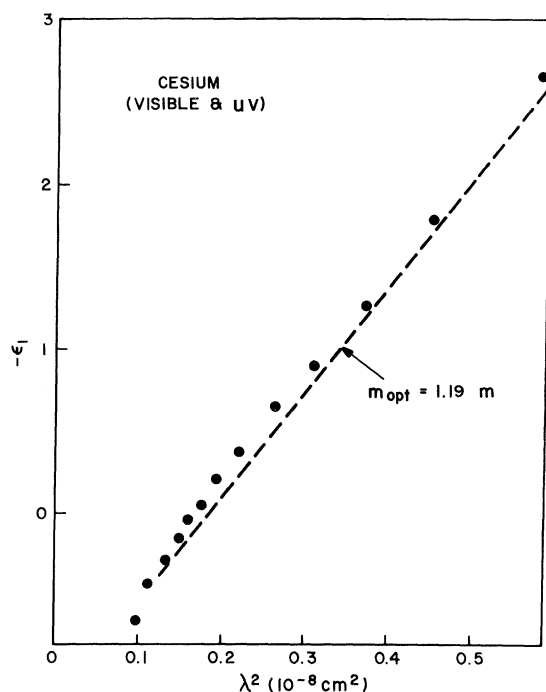


FIG. 9. Real part of the dielectric constant of cesium in the visible and near ultraviolet. The dashed line is a continuation of the line in Fig. 7.

10. It is seen that in Na, K, and Rb, $\sigma(\omega)$ starts to rise in the vicinity of $\hbar\omega/E_F = 0.64$ and shows a peak at about $\hbar\omega/E_F = 1.0$. The results on these metals are in agreement, at least qualitatively, with the nearly-free-electron model. The results on Cs do not fit this picture since the threshold is significantly lower than $0.64E_F$. It has been suggested that this may be associated with the close proximity to the Fermi level of the high-lying d bands in the heavier alkali metals, particularly Cs.

In principle, it should be possible to extract values for the pseudopotential coefficient $|V_{110}|$ in Na, K, and Rb by fitting Eqs. (4)–(6) to the $\sigma(\omega)$ data. A detailed statistical analysis of this kind has been performed on the author's data for Na and K by Powell²¹ using the Gurzhi²² modification of $1/\tau$ in Eq. (5). Powell's values for $|V_{110}|$ are listed in Table III together with the rough estimate for Rb made by the author. Also shown are the values for $|V_{110}|$ extracted by Ashcroft¹¹ from de Haas–van Alphen (dHvA) data. The optical values of $|V_{110}|$ are seen to differ from the dHvA values. In Na, the optical $|V_{110}|$ is larger than the dHvA value, whereas in K and Rb it is the other way round. This is consistent with recent work by Animalu.²³ Animalu and Harrison²⁴ have shown that when wave-function orthogonalization terms

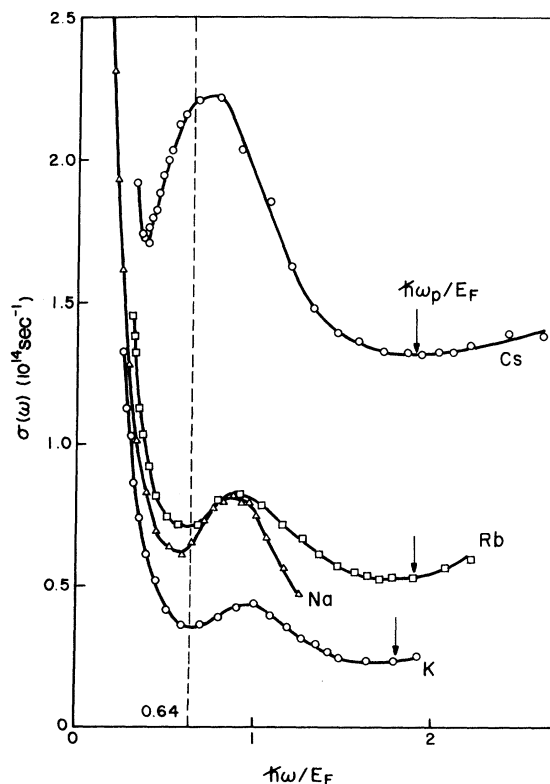


FIG. 10. Optical conductivity of the four alkali metals Na, K, Rb, and Cs plotted against the normalized frequency $\hbar\omega/E_F$, where E_F is the free-electron Fermi energy.

are taken into account, $|V_{110}|$ in Eq. (6) should be replaced by an "optical pseudopotential" equal to $|V_{110} + \hbar\omega P_{110}|$. P_{110} is the matrix element of the projection operator of pseudopotential theory and is positive in sign. The sign of V_{110} therefore

TABLE III. Pseudopotential coefficients (in eV).

	Na	K	Rb
Optical $ V_{110} $			
Powell's analysis ^a of Smith's data	0.30	0.15	(0.26) ^b
dHvA $ V_{110} $ Ashcroft ^c	0.23	0.23	0.43
Theoretical V_{110} Ham ^d	0.11	-0.22	-0.38

^aSee Ref. 21.

^bEstimated by the author as explained in the text.

^cSee Ref. 11.

^dCalculated by Ham (Ref. 10) from the band gap between N_1' and N_1 .

becomes crucial. If V_{110} is positive, as is believed to be the case in Na, then the two terms in the optical pseudopotential reinforce each other, leading to an enhancement of the absorption. If, on the other hand, V_{110} is negative, then the two terms interfere destructively, giving rise to a suppression of the absorption. The observation that the optical $|V_{110}|$ is less than the dHvA $|V_{110}|$ in K and Rb may therefore be an indication that V_{110} is indeed negative in these metals. The negative sign is also suggested by the disposition of s - and p -like character of the states at N in Ham's band calculations.^{10,12} The estimates of V_{110} obtained by Ham from the band gap at N are shown for comparison in Table III. Alternative explanations for the differences between the optical and dHvA values of $|V_{110}|$ are discussed by Powell.²¹ Of course, further optical experiments would be desirable to test whether these differences are really significant.

The plasma frequencies of K, Rb, and Cs are indicated in Fig. 10 by vertical arrows. The rise in the absorption near the plasma frequency which we have already noted in Rb and Cs can also be seen in K. It was not possible to detect whether this effect occurs in Na because the upper limit on the experimental frequency range (4.0 eV) was too far below the plasma frequency (5.7 eV). However, measurements of ϵ_2 above the plasma frequency have been made recently on Na and K by Sutherland, Hamm, and Arakawa²⁵ using a transmission method. They find that ϵ_2 levels off above the plasma frequency in both metals, indicating the onset of some new absorption. Thermorefectance measurements on K, Rb, and Cs by Matatagui and Cardona²⁶ have also revealed structure in the optical absorption above the plasma frequency. Evidence is therefore accumulating from several directions for the existence of this additional absorption near and above the plasma frequency. It is possibly due to one or more of the many-body effects which have been proposed¹⁵⁻¹⁷ to contribute to the optical absorption of the alkali metals. However, as mentioned earlier, we must also consider the possibility that this extra absorption is due to transitions to d bands which are believed to lie not too far above the Fermi level in the heavier alkali metals.

B. Optical Mass

The infrared optical masses extracted from ϵ_1 measurements by the author and by Hodgson²⁷ are listed in Table IV for Li, Na, K, Rb, and Cs. They are compared with the masses obtained in electronic specific-heat measurements²⁸ and cyclotron-resonance experiments.²⁹ The infrared optical masses are seen to be consistently lower than the specific-heat masses or cyclotron masses. There

are theoretical reasons for supposing that this should be the case. The electronic mass measured in a low-frequency experiment such as specific-heat measurement or cyclotron resonance is enhanced by "dressing" effects due to the electron-phonon and electron-electron interactions.³⁰ At optical frequencies, the electrons are oscillating faster than the lattice can follow and so are able to shake off their phonon clothing and quite likely their electron-electron dressing also. The observed difference between the low- and high-frequency masses of Table IV is, therefore, a measure of the dressing effects.

Also shown in Table IV are the theoretical optical and thermal masses calculated by Ham.¹⁰ These two masses are different since they involve different averages over the Fermi surface. It should be emphasized that they are "bare" masses and do not contain the electron-phonon or electron-electron dressing factors mentioned above. The dressing effects are reflected in that the experimental specific-heat masses are greater than the theoretical thermal masses, with the exception of Cs. The theoretical mass in Cs is most likely in error here, since Okumura and Templeton³¹ have shown in de Haas-van Alphen work that Ham's calculations overestimate the distortions of the Fermi surface from sphericity and will consequently overestimate the band mass.

Note that, with the exception of Cs again, the measured optical masses are greater than the theoretical optical masses. This may represent some residual dressing effect due to electron-electron interactions. It may also be associated with the extra optical absorption at higher frequencies for which evidence has been presented earlier. Any optical transitions at higher frequencies, whatever their origin, must rob oscillator strength from the Drude region and this would manifest itself as an increase in the observed optical mass. We conclude that further investigation of the optical ab-

TABLE IV. Effective-mass ratio m^*/m in the alkali metals.

	Li	Na	K	Rb	Cs
Infrared optical mass					
Smith	...	1.13	1.16	1.16	1.19
Hodgson (Ref. 27)	1.57	1.08	1.18
Specific-heat mass (Ref. 28)	2.19	1.27	1.25	1.26	1.43
Cyclotron mass (Ref. 29)	...	1.24	1.21	1.20	1.44
Ham's band masses					
Optical mass	1.45	1.00	1.02	1.06	1.29
Thermal mass	1.66	1.00	1.09	1.21	1.76

sorption at high frequencies ($\hbar\omega > 4$ eV), both experimentally and theoretically, should prove most interesting.

Note added in proof. The extra absorption above the plasma frequency has recently been observed quite clearly in Cs by U.S. Whang, E. T. Arakawa, and T. A. Callcott [Phys. Rev. Letters 25, 646 (1970)].

ACKNOWLEDGMENT

I am deeply grateful to Professor William E. Spicer for suggesting this program of optical work on the alkali metals and for placing the facilities of his laboratory at my disposal.

[†] Part of this work was performed while the author was a research associate at Stanford University, and part while on assignment at Stanford from Bell Telephone Laboratories. The facilities used at Stanford are supported in part by The Advanced Research Projects Agency through the Center for Materials Research at Stanford University and by the National Science Foundation.

* Permanent address.

¹N. V. Smith, Phys. Rev. 183, 634 (1969).

²H. Mayer and M. H. el Naby, Z. Physik 174, 289 (1963).

³H. Mayer and B. Hietel, in *Proceedings of the International Colloquium on Optical Properties and Electronic Structure of Metals and Alloys, Paris*, 1965, edited by F. Abelès (North-Holland, Amsterdam, 1966), p. 47.

⁴N. J. Harrick, *Internal Reflection Spectroscopy* (Interscience, New York, 1967).

⁵N. V. Smith and W. E. Spicer, Phys. Rev. 188, 593 (1969).

⁶Supplied by Atomergic Chemetals Co., Cerle Place, L. I., N. Y.

⁷This formula applies only in the limit $\omega\tau \gg 1$, a condition which is well satisfied in the frequency range under discussion.

⁸A. H. Wilson, *The Theory of Metals* (Cambridge U. P., New York, 1936), p. 133.

⁹P. N. Butcher, Proc. Phys. Soc. (London) A64, 50 (1951).

¹⁰F. S. Ham, Phys. Rev. 128, 2524 (1962).

¹¹N. W. Ashcroft, Phys. Rev. 140, A935 (1965).

¹²F. S. Ham, Phys. Rev. 128, 82 (1962).

¹³For discussion see H. G. Drickamer, in *Solid State Physics*, edited by F. Seitz and D. Turnbull (Academic, New York, 1965), Vol. 17, p. 1.

¹⁴C. Kunz, Z. Physik 196, 311 (1966).

¹⁵J. J. Hopfield, Phys. Rev. 139, A419 (1965).

¹⁶R. J. Esposito, L. Muldower, and P. E. Bloomfield, Phys. Rev. 168, 744 (1968).

¹⁷L. Hedin, B. Lundqvist, and S. Lundqvist, in *Pro-*

ceedings of the Electronic Density of States Symposium, National Bureau of Standards, Gaithersburg, Maryland, 1969 (unpublished).

¹⁸St. von Aufschnaiter, quoted by F. Abelès, in *Soft X-ray Band Spectra* edited by D. J. Fabian (Academic, New York, 1968), p. 191. I am grateful to P. Harms of the Technischen Universität, Clausthal, Germany, for supplying me with these data in numerical form.

¹⁹H. E. Ives and H. B. Briggs, J. Opt. Soc. Am. 27, 395 (1937).

²⁰M. H. Cohen, Phil. Mag. 3, 762 (1958).

²¹C. J. Powell, Opt. Commun. 2, 87 (1970).

²²R. N. Gurzhi, Zh. Eksperim. i Teor. Fiz. 35, 965 (1958) [Soviet Phys. JETP 8, 673 (1959)].

²³A. O. E. Animalu, Phys. Rev. 163, 557 (1967).

²⁴A. O. E. Animalu and W. A. Harrison, Bull. Am. Phys. Soc. 12, 415 (1967).

²⁵J. C. Sutherland, R. N. Hamm, and E. T. Arakawa, J. Opt. Soc. Am. 59, 1581 (1969).

²⁶E. Matatagui and M. Cardona, Solid State Commun. 6, 313 (1968).

²⁷J. N. Hodgson, in *Proceedings of the International Colloquium on Optical Properties and Electronic Structure of Metals and Alloys, Paris*, 1965, edited by F. Abelès (North-Holland, Amsterdam, 1966), p. 60; J. Phys. Chem. Solids 24, 1213 (1963); Phys. Letters 7, 300 (1963).

²⁸W. H. Lien and N. E. Phillips, Phys. Rev. 133, A1370 (1964); D. L. Martin, Proc. Roy. Soc. (London) A263, 378 (1961); Phys. Rev. 124, 438 (1961); J. D. Filby and D. L. Martin, Proc. Roy. Soc. (London) A284, 83 (1965).

²⁹C. C. Grimes and A. F. Kip, Phys. Rev. 132, 1991 (1963); C. C. Grimes, G. Adams, and P. H. Schmidt, Bull. Am. Phys. Soc. 12, 414 (1967).

³⁰D. Pines and P. Nozières, *The Theory of Quantum Liquids* (Benjamin, New York, 1966), Vol. I, p. 336.

³¹K. Okumura and I. M. Templeton, Proc. Roy. Soc. (London) A287, 89 (1965).